

Photocatalytic degradation of methyl parathion: Reaction pathways and intermediate reaction products

Edgar Moctezuma^{a,*}, Elisa Leyva^a, Gabriela Palestino^a, Hugo de Lasa^b

^a Facultad de Ciencias Químicas, Universidad Autónoma de San Luis Potosí, Av. Manuel Nava # 6, San Luis Potosí, S.L.P., México 78290

^b Chemical Reactor Engineering Centre, University of Western Ontario, London, Ont., Canada N6A5B9

Received 23 May 2006; received in revised form 18 July 2006; accepted 24 July 2006

Available online 28 July 2006

Abstract

The photocatalytic degradation of *O,O*-dimethyl *O-p*-nitrophenyl phosphorothioate (common name methyl parathion) in aqueous TiO₂ suspensions is reported in this study. The aim of this article is to identify the intermediate organic reaction products using a number of analytical techniques, such as UV–vis, HPLC, GC–MS and ¹H NMR. Total organic carbon (TOC) and the concentration of inorganic ions in the reaction mixture, as a function of reaction time, are also measured to monitor the mineralization of organic chemical species. Under both, acidic and basic conditions, the primary product is methyl paraoxon, which eventually is degraded to 4-nitrophenol. This aromatic compound is mainly transformed into hydroquinone, which is later oxidized to 1,2,4-benzenetriol. GC–MS studies show that this aromatic triol is preferentially converted via an oxidative pathway into 5-hydroxymethyl-5H-furfuran-2-one. Under basic conditions, methyl parathion is converted via a reaction pathway involving methyl paraoxon, 4-nitrophenol, hydroquinone and aliphatic acids with the resulting species being refractory to be further oxidized and mineralized. On the other hand, under controlled acidic conditions, methyl parathion and various intermediates quickly degrade in a rather fast oxidation process.

© 2006 Elsevier B.V. All rights reserved.

Keywords: Photocatalytic oxidation; Organophosphorous pesticides; Methyl parathion; Titanium dioxide

1. Introduction

Photocatalysis on a semiconductor is an advanced oxidation process used to remove organic pollutants from water. In the last few years, there have been a number of studies and reviews about this process [1–3]. Photocatalytic oxidation is based on the use of UV light and a semiconductor. Titanium dioxide has become the most studied and used photocatalyst. TiO₂ is easily available, chemically robust and durable. It can be used to degrade, via photocatalysis, a wide range of organic compounds [4–9].

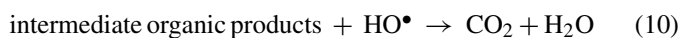
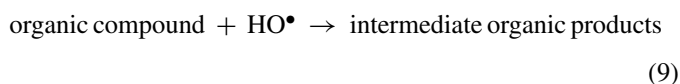
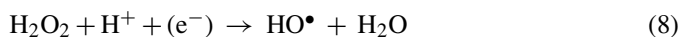
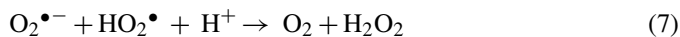
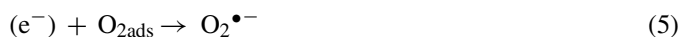
Photocatalytic oxidation reactions are initiated when a photon of energy higher or equal to the bandgap energy is absorbed by a semiconductor catalyst promoting an electron (e⁻) from the valence band to the conduction band with simultaneous generation of a positive hole (h⁺) in the valence band [1–3]. Most of

the e⁻ and h⁺ recombine in a few nanoseconds and the energy is dissipated as heat. Only a few of the electrons (e⁻) and holes (h⁺) migrate to the surface of the catalyst where they initiate oxidation and reduction reactions. In an aqueous suspension, positive holes (h⁺) react with adsorbed water and OH⁻ groups to give strong oxidizing HO• radicals. In addition, the free electrons (e⁻) react with adsorbed molecular O₂ to produce O₂•⁻ superoxide anions that may also contribute to the production of HO• radicals through the formation of HO₂• radicals and H₂O₂. It is believed that the reaction of the HO• radicals with organic pollutants is a key reaction step leading to mineralization of these compounds [10]. Indeed electron spin resonance studies have demonstrated that HO• is the most abundant radical species in aqueous TiO₂ suspensions [11]. Thus, the above-mentioned photocatalytic oxidation of organic pollutants can be described via the following reaction sequence [1–3,11]:



* Corresponding author at: Chemical Reactor Engineering Centre, CREC, University of Western Ontario, London, Ont., Canada N6A 5B9 (on sabbatical leave from UASLP). Tel.: +1 519 661 2111x88218; fax: +1 519 850 2931.

E-mail addresses: emoctezu@uwo.ca, edgar@uaslp.mx (E. Moctezuma).



Many publications on photocatalysis focus on the practical aspects of this technique for the clean up of contaminated waters [1,3,8]. Others are more concerned with the effect of experimental parameters on the initial rate of disappearance or the total mineralization rate of organic pollutants [5,7]. Finally, there is a group of studies addressing the more fundamental aspects of reaction mechanisms and the pathways by which organic pollutants are degraded to CO_2 and H_2O [6,8–18].

Organophosphorous compounds OPC are organic pollutants extensively used as insecticides since they are known to inhibit acetylcholinesterase [19]. Most of them are highly toxic for human beings and mammals [20]. In the environment, they are slowly hydrolyzed to other toxic chemical species [21] but they are quite persistent in water solution [22].

There are several methods to remove OPC from water but each method has its shortcomings [23]. Chemical oxidation is expensive and leads to the contamination of water with other toxic pollutants. Biodegradation can only be used with diluted wastewaters. Therefore, photocatalysis on semiconductors seems to be an ideal method for removal of pesticides since it is rapid and non-selective.

Methyl parathion MP and ethyl parathion EP are non-systemic OPC insecticides and acaricides. Despite their high degree of toxicity, they are the most commonly used pesticides. Roques [24] reported that EP in aqueous solution can be mineralized by ozonation. However, In order to achieve complete oxidation a high concentration of ozone is required.

The photochemical degradation of EP in aqueous solutions under different reaction conditions has been investigated [25–27]. It was reported that light from a xenon arc lamp ($240 < \lambda < 320$ nm) is required to induce the photochemical reactions. Furthermore, the rate of degradation increases with pH. Pignatello and Sun [28] reported the complete oxidation of MP in water using the UV photoassisted Fenton reaction in an aqueous solution containing MP, Fe^{3+} and H_2O_2 . Under these conditions, MP yields quantitatively HNO_3 , H_2SO_4 and H_3PO_4 , with oxalic acid, 4-nitrophenol and dimethylphosphoric acid being the organic identified intermediate species.

O'Shea et al. [29] demonstrated that TiO_2 photocatalytic degradation of an OPC type insecticide, dimethyl methyl

phosphonate (DMMP), can be accomplished in oxygenated aqueous solutions. Final products of the DMMP degradation are phosphoric acid and CO_2 . On the other hand, Malato et al. [30] demonstrated that TiO_2 photocatalyzed mineralization of methamidophos occurs in aqueous solutions under solar irradiation. Total organic carbon (TOC) and PO_4^{3-} contents were analyzed to confirm the extent of mineralization.

Doong and Chang [31] studied the photooxidation of several OPC such as methamidophos, malathion and diazion using UV- TiO_2 , UV- H_2O_2 , and UV- TiO_2 - H_2O_2 mixtures. The addition of H_2O_2 to the reaction mixture resulted in a more efficient photocatalytic degradation process. Even more, Kerzhentsev et al. [32] analyzed the photocatalytic oxidation of fenitrothion using TiO_2 suspensions. They detected several intermediate organic compounds that were completely mineralized to CO_2 , $H_2PO_4^-$, SO_4^{2-} and NO_3^- .

Konstantinou et al. [33] investigated the photocatalytic oxidation of several other OPC (ethyl parathion, methyl parathion, dichlorofenthion and ethyl bromophos) in aqueous TiO_2 suspensions. Some of the major intermediate products of photodegradation were identified by means of MS. In a more recent study, Sakkas et al. [34] reported the application of solid-phase microextraction for monitoring the photocatalytic decomposition of EP in aqueous TiO_2 suspensions. Some of the intermediate organic reaction products were successfully extracted with this technique and identified by combined GC-MS.

Sanjuán et al. [35] described the use of 2,4,6-triphenylpyrylium ion encapsulated within Y zeolite as a photocatalyst for the photodegradation of methyl parathion in aqueous suspensions. Encapsulation stabilizes the pyrylium ion leading to degradation efficiencies comparable to those obtained with TiO_2 . It was suggested that radical intermediates are involved in the degradation process.

The photocatalytic degradation of various aromatic compounds has been previously carried out in our laboratories with the aim of evaluating the efficiency of the process and determining the factors that modify this reaction [1,5,7]. Our research group has reported preliminary mechanistic studies concerning the TiO_2 photocatalytic degradation of methyl parathion [36,37]. In spite of the several publications available in the literature, there is still the need of the determination of a comprehensive reaction mechanism for the photocatalytic mineralization of methyl parathion using as a basis the experimentally detectable chemical species. In the present study, the photocatalytic degradation of MP was monitored using different complementary analytical techniques to identify the organic intermediates and to follow their evolution. Total organic carbon (TOC) and concentration of inorganic ions present in the reaction mixture were also measured to obtain information about the progress of the reaction and the extent of mineralization. To accomplish these goals, combined UV and NMR identification techniques were employed performing the photocatalytic degradation of MP in D_2O . To the best of our knowledge, this is the first comprehensive study providing detailed insights and understanding of the MP degradation reaction pathways.

2. Experimental

2.1. Materials

Methyl parathion technical grade (79.4% purity) donated by Bayer was used in the present studies without further purification. Phenol, 4-nitrocatechol, 1,2,4-benzenetriol, 4-nitroanisole, 4-nitrophenol, hydroquinone and benzoquinone were purchased from Aldrich and methyl paraoxon from Riedel-de Haen. Several organic and inorganic acids and salts used in the product studies were purchased from J.T. Baker. Spectroscopic and chromatographic grade solvents were purchased from Mallinckrodt. Titanium dioxide (Degussa P25), provided by Degussa Co., a known mixture of 80% anatase and 20% rutile with a 30 nm average particle size, a non-porous material with a 50.10 m²/g reactive area was used as received for the photodegradation experiments. Double distilled water, filtered through 0.45 μm HA cellulose acetate membranes (Millipore Corp. Bedford, MA) was used throughout. Before analysis, all the reaction mixtures were filtered through 0.22 μm GV cellulose acetate membranes (Millipore Corp. Bedford, MA).

2.2. Analytical methods

For the determination of MP and intermediate organic compounds, the samples were analyzed by high performance liquid chromatography (HPLC) in a 600E Waters instrument equipped with a UV Waters 490 detector. A Supelco C-18 column (150 mm × 3.9 mm × 5.0 μm) was used for separation of reactant and product intermediates. The mobile phase was a mixture of acetonitrile and water (60/40) filtered through a 0.22 μm HA cellulose acetate Millipore membrane. The elute was delivered at a rate of 1.5 mL/min and the wavelength of detection was 276 nm. For these operating conditions, the retention times for methyl parathion, methyl paraoxon, 4-nitrophenol, hydroquinone and aliphatic acids were 3.3, 1.54, 1.39, 1.24 and 0.78 min, respectively. The analytical error was controlled within 5%. The total organic carbon (TOC) in some samples was measured with a Shimadzu carbon analyzer model 5000 A.

For the determination of inorganic anions, the samples were analyzed by HPLC in a 526 Alltech instrument with a 550 Alltech conductivity detector using an Allsep ion 7u column with an ERIS 1000 HP precolumn. The mobile phase was a solution of sodium bicarbonate (0.85 mM) and sodium carbonate (0.90 mM) filtered through a 0.22 μm HA cellulose acetate Millipore membrane. The elute was delivered at a rate of 1.2 mL/min. A certified Alltech kit of anions was used as standard. For these operating conditions, the retention times for formate (HCOO⁻), nitrite (NO₂⁻), nitrate (NO₃⁻), phosphate (PO₄³⁻) and sulfate (SO₄²⁻) were 3.06, 5.21, 8.6, 12.05, and 13.65 min, respectively. For quantitative studies, standard solutions and calibration curves for each ion were prepared in the range from 2 to 50 ppm. In order to study the adsorption of phosphate ions (PO₄³⁻) on the catalyst surface, some of the reaction samples were pre-treated with a NaOH solution (3N) before chemical analysis.

Some of the reaction mixtures were monitored via UV–vis spectroscopy in a Shimadzu UV-2401 PC instrument in standard quartz cells. Other samples were analyzed by ¹H NMR spectroscopy in a Bruker NMR model AC 200. To identify the intermediate organic species, some samples were analyzed by GC–MS in a HP 6890 instrument with a HP 5973 detector. A capillary HP-5MS column (5% phenylmethylsiloxane, 60 m × 250 μm × 0.25 μm) was used to separate the components of the mixture. The carrier gas used was Helium at a rate of 25 mL/min. The system was operated with initial temperature of 50 °C, then the temperature was increased 8 °C/min up to 234 °C, then the temperature was increased 5 °C/min up to 320 °C. Before analysis, an aliquot of the reaction mixture (5 mL) was extracted with ethyl acetate (5 mL), dried over anhydrous sodium sulfate and filtered.

2.3. Photoreactor and photodegradation experiments

Photocatalytic degradation experiments were carried out in a reactor system already described in previous publications [36,38,39]. This unit is configured with a Pyrex glass tube reactor (200 mL) irradiated with four 15 W UV light lamps (Cole-Parmer E-09815-55, λ_{max} = 365 nm). For each set of experiments, 100 mL of a MP standard solution were placed inside the glass reactor and slurried with 0.2 g of TiO₂. This suspension was mixed with a magnetic stirrer and pure oxygen, air or an inert gas was bubbled through the system at a constant rate of 100 mL/min. A standard solution was prepared by mixing 40.8 μL of MP (ρ = 1.223 g/mL) in 1 L of water. Prior to the experiments, the suspension was agitated in an ultrasonic bath for 15 min under dark to dissolve all the MP. Under these conditions, the initial pH of the solution measured using a 710A Orion pH meter was 4.5 ± 0.2. Samples were taken from time to time to monitor the progress of the photoreaction. Before analysis, each sample was filtered with a Millipore GV membrane (0.22 μm of pore diameter).

Furthermore and in order to unambiguously identify the organic reaction intermediate species, NMR analysis, a special feature of this study versus previous contributions [34,35], was effected. Two MP solutions (300 and 50 ppm) in deuterated water were photolyzed using 0.2 g of TiO₂ per 100 mL of D₂O. For the first experiment, aliquots (5 mL) were taken at different time intervals and extracted with deuterated chloroform (5 mL). The organic phase was dried over anhydrous sodium sulfate, filtered and placed in a NMR tube for analysis. For the second experiment, samples of 1 mL were taken at different time intervals, filtered and analyzed by UV–vis spectroscopy and HPLC.

Regarding experiments with deuterated water, it is expected that D₂O may reduce OH• availability. Thus, the rates of the MP degradation steps, later described in this study and all of them OH• promoted, are influenced by the use of D₂O. It is anticipated however, that these changes in OH• concentrations while affecting various step rates do not alter the sequence of chemical changes in the network. As a result, the MP photodegradation in D₂O provides a valuable approach for the establishment of the reaction network via the identification of both organic intermediates and inorganic anion species.

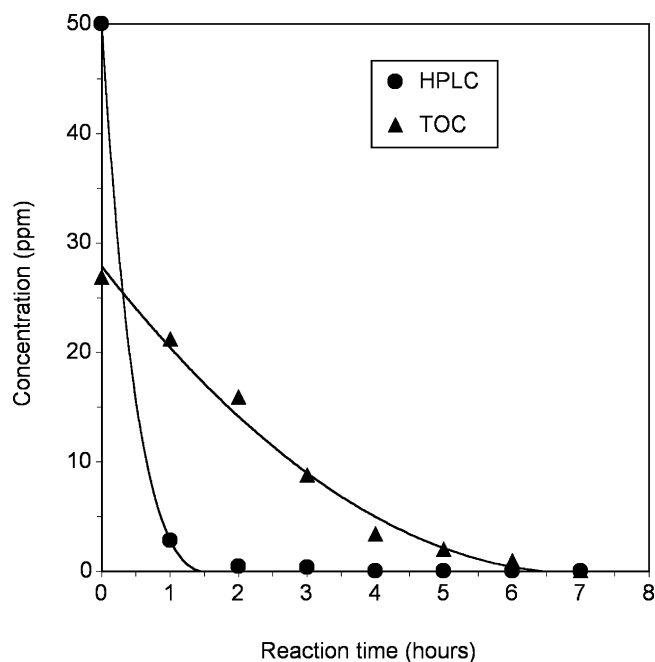


Fig. 1. Photocatalytic degradation of methyl parathion with TiO_2 and UV light. ($V = 100 \text{ mL}$, $C_0 = 50 \text{ ppm}$, $\text{TiO}_2 = 0.2 \text{ g}/100 \text{ mL}$, four UV lamps, $\lambda_{\text{max}} = 365 \text{ nm}$, oxygen flow = $100 \text{ mL}/\text{min}$.)

3. Results and discussion

3.1. TOC and HPLC studies

A preliminary experiment was carried out to study the photocatalytic degradation of MP in aqueous solution (50 ppm) with TiO_2 (0.2 g/100 mL of solution), UV light and a flow of 100 mL/min of pure oxygen. The composition changes in the reaction mixture were monitored by both HPLC and TOC (Fig. 1). Experimental HPLC results show that MP is quickly oxidized into other organic compounds. TOC results also show that the intermediate organic species remain in the solution for several hours and are eventually mineralized into CO_2 and H_2O . Comparing HPLC and TOC curves it is apparent that the organic intermediate species degrade at a much slower rate than methyl parathion.

3.2. Influence of operating parameters on the photocatalytic degradation of MP

Various parameters such as, amount of catalyst, concentration of dissolved oxygen and pH have a strong effect on the photocatalytic degradation rate of organic compounds [1,8]. The photocatalytic oxidation of MP in aqueous solution (50 ppm) with different TiO_2 catalyst concentrations (0.1, 0.2 or 0.4 g/100 mL of solution) was investigated. In the range studied, the effect of TiO_2 concentration was quite small and within experimental error (5%). Since the main interest on the present study is to monitor the intermediate species generated in this photocatalytic process with the aim of unveiling the photoreaction mechanism, it was decided to keep the amount of catalyst at a constant value (0.2 g/100 mL) during all the experiments performed.

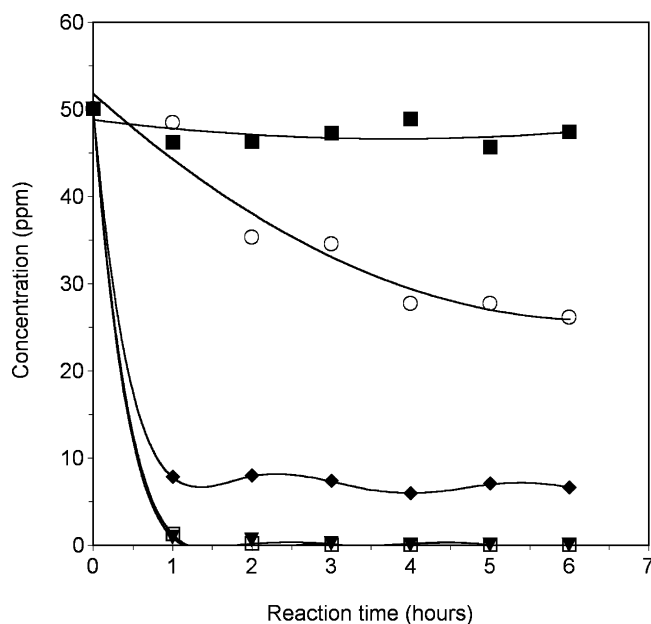
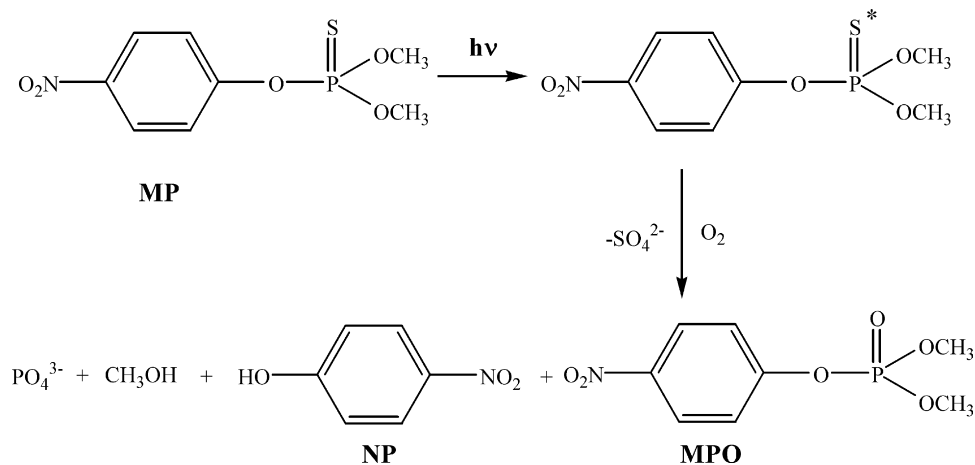


Fig. 2. Photocatalytic degradation of methyl parathion under different reaction conditions. ($V = 100 \text{ mL}$, $C_0 = 50 \text{ ppm}$). (■) Inert gas flow + near UV light, (○) airflow + near UV light, (◆) air saturated + near UV light + TiO_2 Degussa P25, (□) airflow + near UV light + TiO_2 Degussa P25, (▼) oxygen flow + near UV light + TiO_2 Degussa P25.

The degradation of MP (50 ppm) in aqueous solution was also studied under several reaction conditions: (a) inert gas flow, irradiated solution and no TiO_2 addition, (b) airflow, irradiated solution and no TiO_2 addition, (c) TiO_2 added, irradiated and air saturated water solution, (d) airflow, TiO_2 added and irradiated solution and (e) oxygen flow, catalyst added and irradiated solution (Fig. 2). It was observed that while nitrogen gas was bubbled in water solution under near-UV light ($\lambda_{\text{max}} = 365 \text{ nm}$) illumination no reaction was observed. In contrast, when the water solution was saturated with air, the dissolved oxygen helped achieve up to 48% conversion showing that molecular oxygen plays an essential role in photochemical transformations. These results are consistent with previous reports on the photochemical degradation of EP to ethyl paraoxon and 4-nitrophenol under UV irradiation [25–27]. It is hypothesized that this photodegradation involves an excited MP^* molecule as a key intermediate, with intermediates undergoing further oxidative transformation to methanol, sulfate, phosphate, methyl paraoxon and 4-nitrophenol (Scheme 1). MP or EP absorbs radiation with wavelengths shorter than 320 nm. Consistent with this, low conversion of MP (<50%) was obtained under the near-UV irradiation provided by the lamps used in the present study ($\lambda_{\text{max}} = 365 \text{ nm}$).

As expected for a photocatalytic process (Fig. 2), a strong enhancement in the oxidation reaction was observed in the presence of TiO_2 (0.2 g/100 mL). However, the photocatalytic mineralization of MP is arrested unless enough dissolved oxygen is available in the solution. To accomplish this, a constant oxygen flow rate of 100 mL/min was used during the experiments. Similar degradation rates were observed when the degradation was done employing a constant airflow instead of an oxygen flow.



Scheme 1. Photochemical oxidation of methyl parathion.

Regarding the pH effect, a small influence if any was observed on the photocatalytic degradation of MP monitored by HPLC in the range studied (pH between 3 and 9). On the other hand, the pH had a strong influence on the TOC conversion (Fig. 3). At acidic pH (2–4), a large TOC conversion (90%) was noticed indicating that MP and intermediate species were both mineralized. However, at basic pH (9), only 60% TOC conversion was attained suggesting that intermediate reaction products are only partially oxidized. The photocatalytic degradation of MP at the pH of 4.5 and 9.0 was monitored by HPLC (Figs. 4 and 5) to determine the presence of some of the organic intermediate reaction products. It was then noticed that under highly acidic conditions, methyl parathion and intermediate compounds undergo fast degradation. On the other hand, under basic conditions, the MP degradation is still allowed with the degrada-

tion rate of the formed intermediate species being significantly reduced.

One of the most fundamental questions in photocatalytic degradation, regarding the nature of substrate–catalyst interactions, is whether reactions occur in the homogeneous bulk phase or at the surface of the catalyst. Some investigators have indicated that most reactions occur at the surface [40]. However, since it was observed an inverse relationship between the degradation rate and amount of adsorbed material, it has been argued that degradation at higher initial pH occurs in the bulk water [41]. In other recent publications, it has been suggested that hydroxyl-like chemistry may occur at or near the surface of the catalyst, but it may have less rigorous requirements for specific adsorption modes or sites of adsorption than a classical electron transfer between a substrate and TiO₂ surface [42].

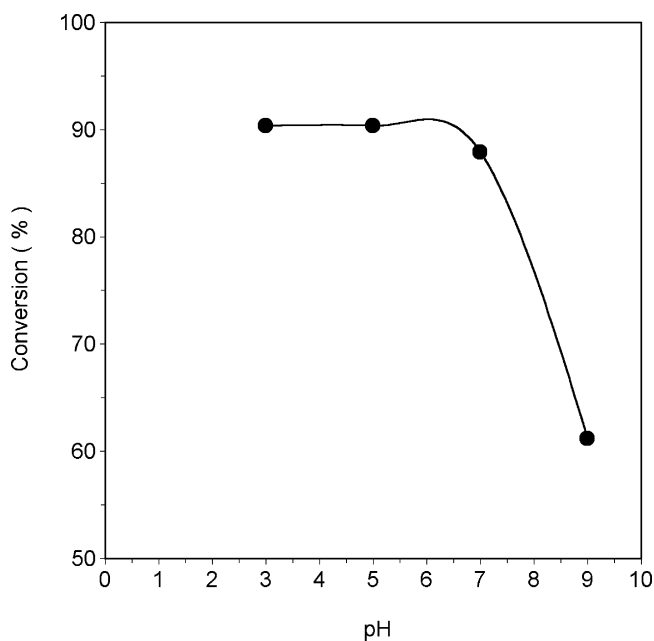


Fig. 3. Effect of pH on the conversion of total organic carbon for the photocatalytic degradation of methyl parathion after 6 h of reaction. ($V=100$ mL, $C_0=50$ ppm, $\text{TiO}_2=0.2$ g/100 mL, four UV lamps, $\lambda_{\text{max}}=365$ nm, oxygen flow = 100 mL/min.)

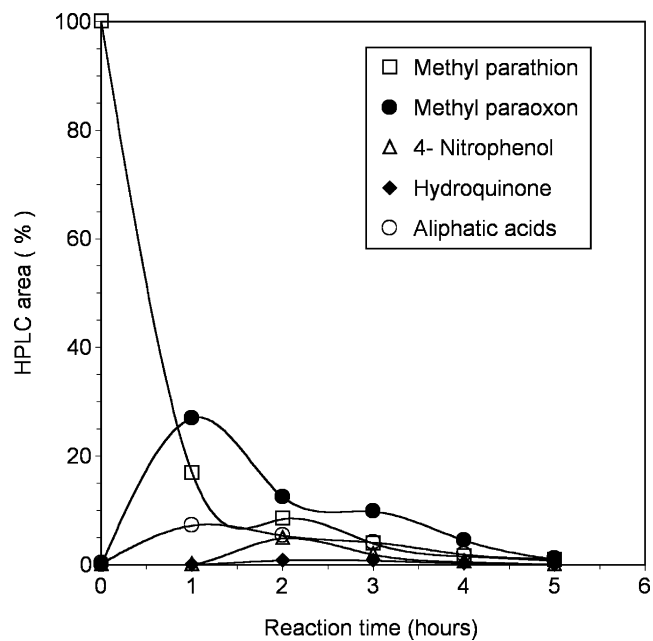


Fig. 4. Photocatalytic degradation of methyl parathion and subsequent formation and disappearance of intermediate organic products as a function of time. (Initial pH 4.5, $V=100$ mL, $C_0=50$ ppm, $\text{TiO}_2=0.2$ g/100 mL, two UV lamps, $\lambda_{\text{max}}=365$ nm, oxygen flow = 100 mL/min.)

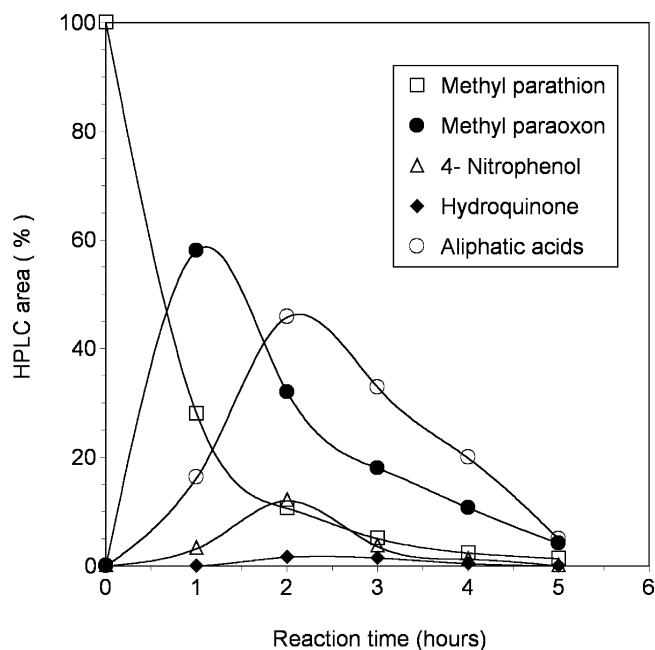


Fig. 5. Photocatalytic degradation of methyl parathion and subsequent formation and disappearance of intermediate organic products as a function of time. (Initial pH 9, $V = 100$ mL, $C_0 = 50$ ppm, $\text{TiO}_2 = 0.2$ g/100 mL, two UV lamps, $\lambda_{\text{max}} = 365$ nm, oxygen flow = 100 mL/min.)

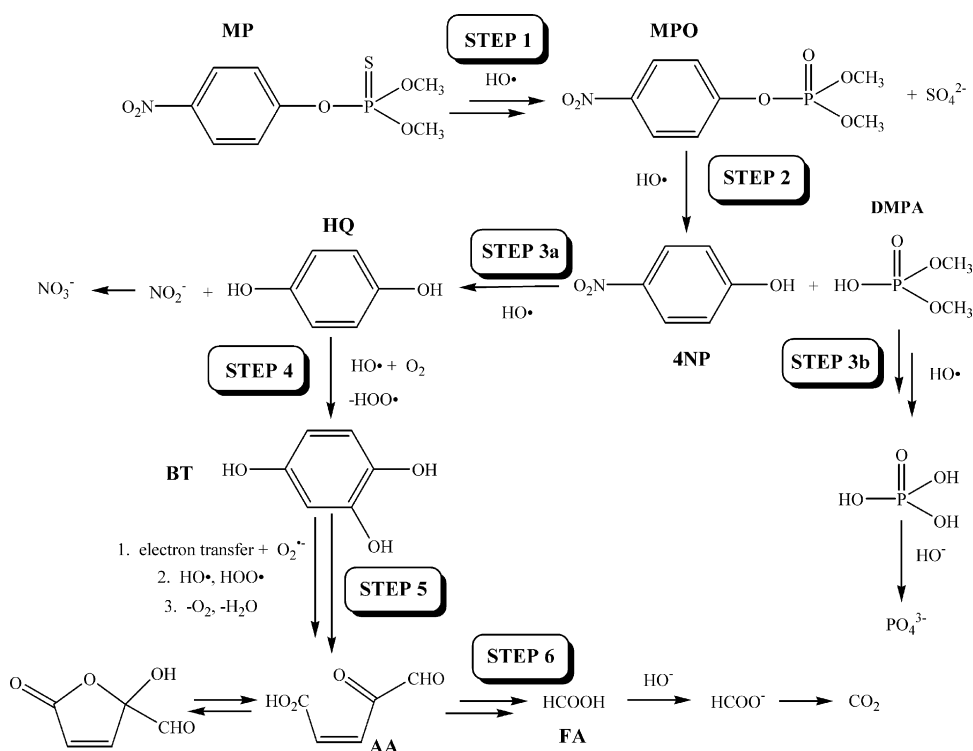
The experimental results of this study also demonstrate that methyl paraoxon is slowly degraded under basic conditions. These results do not agree with previous experimental reports in which the rate of photocatalytic degradation of dimethyl methylphosphonate increased at high pH [29]. It is hypothe-

sized that the strength of attractive interactions between TiO_2 surface and a given phosphonate is modified by its chemical structure. In the case of this study and due to the presence of a large aromatic substituent in paraoxon, one might expect weaker attractive interactions between this organic compound and the surface of TiO_2 .

3.3. MP degradation reaction network

The main objective of the present study is to establish, on the basis of the experimentally identified intermediate species, a suitable reaction mechanism for the degradation of MP. This is a reaction proceeding in the first few steps in series (conversion of the MP into MPO and NP) and later on via two simultaneous sequence of reactions leading in one hand to the mineralization of organic intermediates forming CO_2 and on the other hand to the formation of inorganic SO_4^{2-} , PO_4^{3-} and NO_3^- anions. A reaction network is presented in Scheme 2 based on the experimental data of this study.

Monitoring the intermediate organic species produced on the TiO_2 photocatalytic degradation of MP at pH 4.5 (Fig. 4) it was observed that MP is first oxidized to methyl paraoxon (MPO). In the same reaction mixture, other intermediate compounds, such as 4-nitrophenol (NP) and hydroquinone (HQ) were produced and consumed. Small amounts of aliphatic acids (AA) were also detected in the reaction mixture. These acids are most likely produced by subsequent degradation of aromatic species [12,13]. Therefore, it is concluded that MP is first oxidized to methyl paraoxon (Step 1 in Scheme 2) with MPO being oxidized later (Step 2) to 4-nitrophenol with NP undergoing eventually further oxidation (Steps 3a and 4).



Scheme 2. Proposed overall reaction mechanism for the photocatalytic oxidation of methyl parathion.

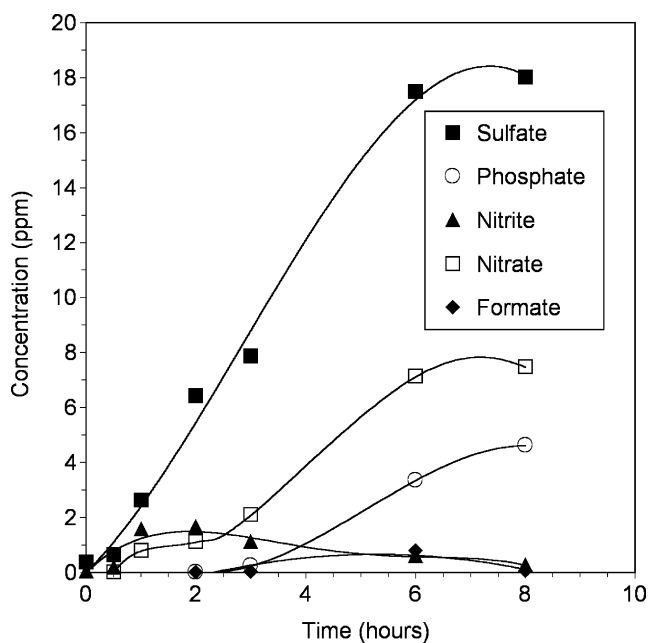


Fig. 6. Formation and disappearance of inorganic anions during the photocatalytic degradation of methyl parathion. (Initial pH 4.5, $V=100$ mL, $C_0=50$ ppm, $TiO_2=0.2$ g/100 mL, two UV lamps, $\lambda_{max}=365$ nm, oxygen flow = 100 mL/min.)

An alternative approach for tracking the progress of the TiO_2 photocatalytic degradation of MP at pH 4.5 (Fig. 6) is to monitor the sulfate anions (SO_4^{2-}) formed in the solution. It is confirmed, in this manner, that there is a quick oxidation of methyl parathion to methyl paraoxon (Step 1 in Scheme 2) with SO_4^{2-} being also formed as a result of this first step of the reaction pathway.

The experiments of this study showed trace amounts of 4-nitrocatechol (NC) and 1,2,4-benzenetriol (BT) only. These findings are consistent with a direct (not sensitized) photocatalytic pathway in which the oxidative degradation of an organic compound is attributed to the reaction with HO^\bullet radicals [43,44]. In spite of the disagreement with a recent theoretical study arguing that 4-nitrocatechol is the most probable primary intermediate in nitrophenol decomposition [45], the experimental data of this study support the postulated Step 3 of Scheme 2 with NP being converted to hydroquinone.

It should also be noticed that nitrogen is given into the solution as nitrite anions (NO_2^-), which are eventually oxidized to the more stable nitrate anions (NO_3^-). Formation of both nitrite anions (NO_2^-) and nitrate anions (NO_3^-) provides additional support to Step 3a of Scheme 2 where NP is converted to HQ.

Even more, the photocatalytic conversion of phenolic compounds in photocatalytic reactors into carboxylic acids (Step 6 of Scheme 2) is also confirmed in the present study via the formation of small amounts of formate anions ($HCOO^-$).

Phosphate anions (PO_4^{3-}), as shown in Fig. 6, were also observed. These results support Step 3b of Scheme 2 that describes the decomposition of di-methyl phosphoric acid. However, phosphate anions were only detected after 3 h of reaction. This delayed increase of phosphate anions concentration is consistent with the findings of other researchers [46] and shows

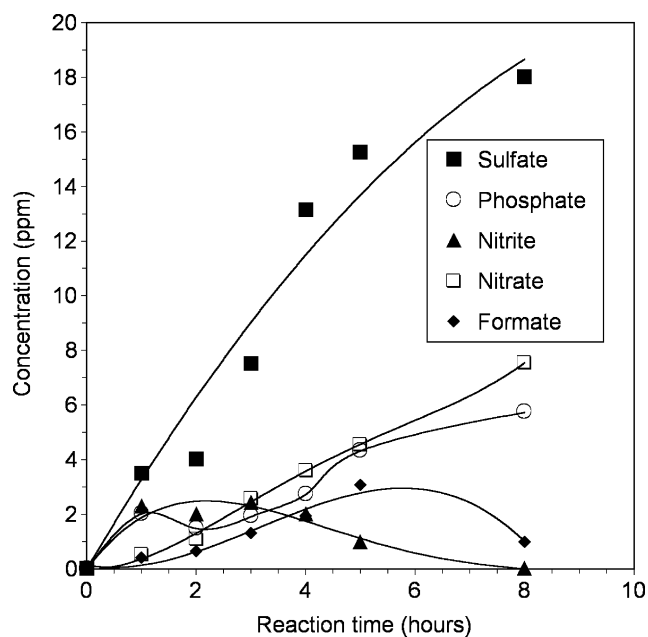


Fig. 7. Formation and disappearance of inorganic anions during the photocatalytic degradation of methyl parathion. Reaction samples were treated with a NaOH solution before analysis. (Initial pH 4.5, $V=100$ mL, $C_0=50$ ppm, $TiO_2=0.2$ g/100 mL, two UV lamps, $\lambda_{max}=365$ nm, oxygen flow = 100 mL/min, reaction samples were treated with a NaOH solution before analysis.)

that phosphate anions are strongly adsorbed on TiO_2 . In order to eliminate the bias of phosphate anions adsorption, the reaction samples were pre-treated with a sodium hydroxide solution (Section 2.2). This alkali promoted phosphate anions desorption prior to the HPLC anion analysis (Fig. 7). This method allowed

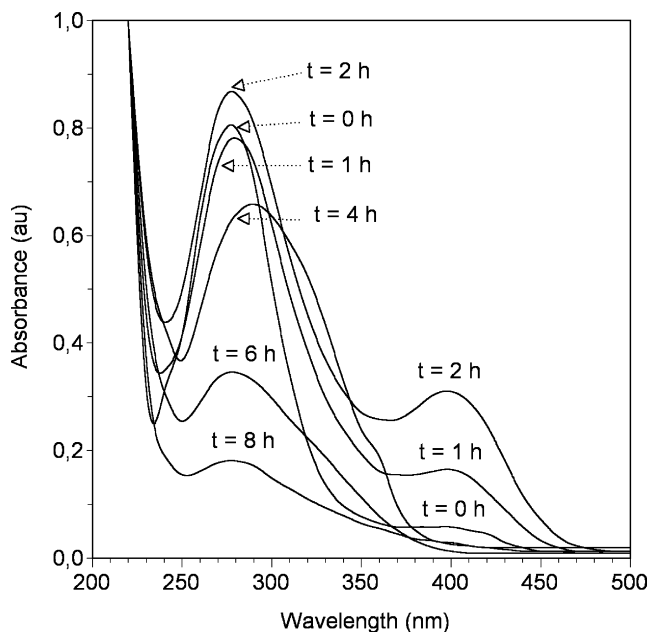


Fig. 8. Photocatalytic degradation of a methyl parathion solution in D_2O using TiO_2 as catalysts. Samples for UV analysis were taken at 0, 1, 2, 4, 6 and 8 h of reaction. (Initial pH 8.0, $V=100$ mL, $C_0=50$ ppm, $TiO_2=0.2$ g/100 mL, two UV lamps, $\lambda_{max}=365$ nm, oxygen flow = 100 mL/min.)

detection of phosphate anions (PO_4^{3-}) concentration up to the level consistent with other photoconversion changes taking place at the early stages of the photodegradation.

3.4. Investigation of MP reaction pathways by means of different analytical techniques

3.4.1. UV-vis spectroscopy

In order to investigate the formation and eventual disappearance of intermediate compounds in the reaction mixture, the photocatalytic reaction of MP dissolved in deuterated water was monitored using UV-vis spectroscopy as a function of time (Fig. 8). The characteristic 4-nitrophenol absorption band at 399 nm [47] was observed to increase upon short time photolysis between 0.5 and 2.0 h. However, upon extended photolysis

(2.0–8.0 h) this same band decreased in intensity and eventually disappeared. Mineralization of aromatic compounds in the reaction mixture was apparent on the UV-vis spectrum of the sample with most of the characteristic absorption bands disappearing after several hours of irradiation.

3.4.2. NMR spectroscopy

NMR was a key analytical tool used in this study to get valuable insights on the structure of intermediate compounds formed in the photocatalytic oxidation of MP. In order to accomplish this, photocatalytic MP degradation experiments were developed using deuterated water with reaction mixture samples being analyzed by NMR. At different reaction times, 5 mL aliquots were removed, extracted with chloroform (5 mL), dried, filtered and placed in tubes to get a ^1H NMR spectrum. Changes in the chemical structure of the components of the reaction mixture were monitored as the photocatalytic degradation reaction proceeded.

At the onset of the experiment (non-irradiated or dark period), samples of a MP (300 ppm) solution displayed the characteristic ^1H NMR signals of this aromatic organophosphorous ester compound. Two signals ($J = 8$ Hz) at 8.24 ppm and 7.32 due to the aromatic hydrogen atoms and two singlet signals at 3.93 and 3.86 ppm due to the two types of methyl hydrogen atoms present in methyl parathion were observed. Since the aromatic signals in the region from 7 to 9 ppm on the NMR spectrum are rather small, Fig. 9a displays the NMR signals in the region from 0.5 to 4.5 ppm only. At room temperature, two strong signals of methyl hydrogen atoms are observed due to the rotation of the phosphate group. Hydrogen atoms

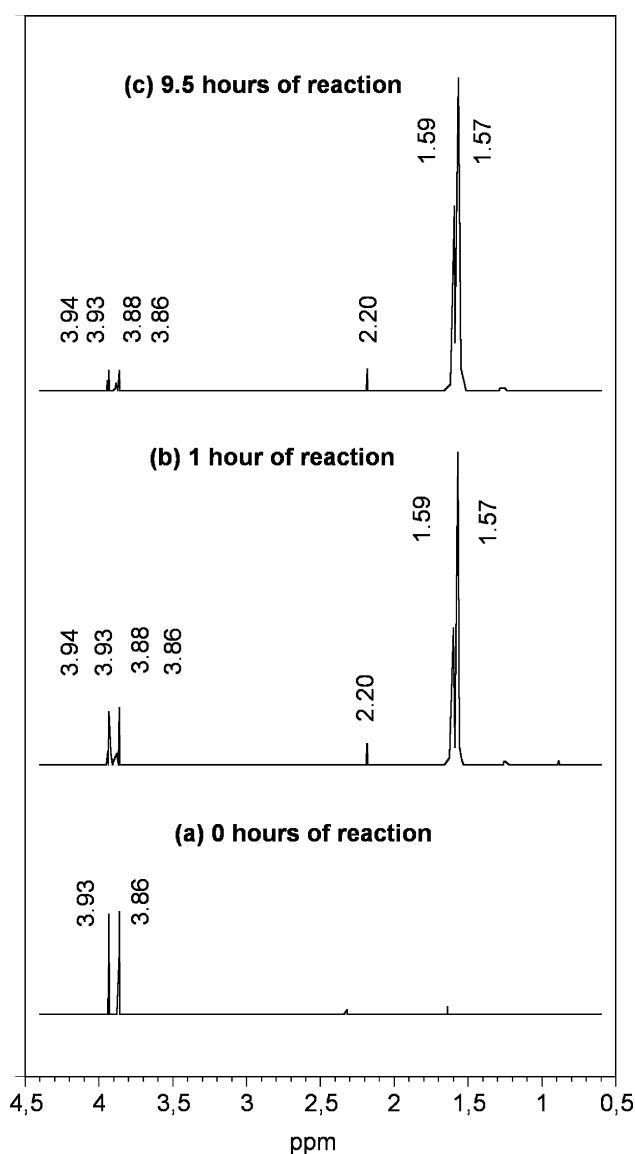


Fig. 9. Photocatalytic degradation of a methyl parathion solution in D_2O using TiO_2 as catalysts. Samples for NMR analysis were taken at 0, 1 and 9.5 h of reaction. (Initial pH 8.0, $V = 100$ mL, $C_0 = 300$ ppm, $\text{TiO}_2 = 0.2$ g/100 mL, two UV lamps, $\lambda_{\text{max}} = 365$ nm, oxygen flow = 100 mL/min.)

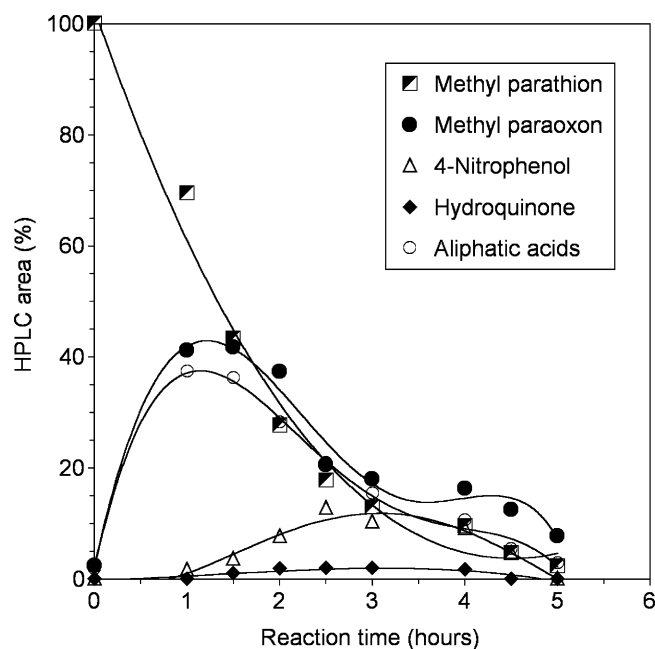


Fig. 10. Photocatalytic degradation of a methyl parathion solution in D_2O and subsequent formation and disappearance of intermediate organic products as a function of time. (Initial pH 8, $V = 100$ mL, $C_0 = 50$ ppm, $\text{TiO}_2 = 0.2$ g/100 mL, two UV lamps, $\lambda_{\text{max}} = 365$ nm, oxygen flow = 100 mL/min.)

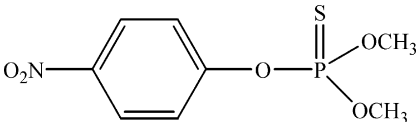
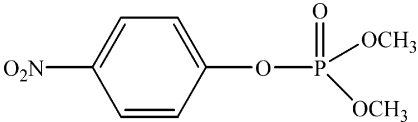
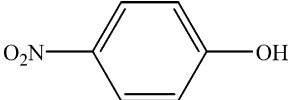
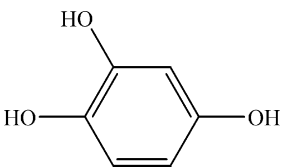
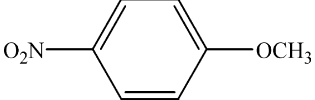

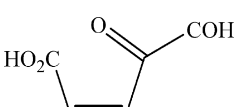
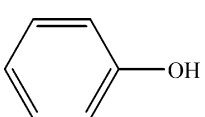
on carbon atoms attached to oxygen (like in $R-O-CH_3$) are strongly deshielded due to the electronegativity of the oxygen atom.

After 1 h of photolysis, the formation of methyl paraxon was observed in the reaction mixture. This was evidenced by changes in two regions of the 1H NMR spectrum. In the aromatic region, four small signals ($J=8$ Hz) at 8.28, 8.24, 7.36, and 7.32 ppm were observed due to the presence of four types of aromatic hydrogen atoms. In addition to this, four different singlet signals (Fig. 9b) were also observed at 3.94, 3.93, 3.88 and 3.86 ppm due to the presence of four $R-O-CH_3$ groups, two for methyl parathion and two for methyl paraxon. Furthermore, strong singlet signals at 1.59 and 1.57 ppm were also detected and evidenced the presence of other $C-H$ groups in the reaction mixture. Signals in this range are characteristic of methyl or methylene groups [47] connected with unsaturated carbon atoms (like $H_3C-C=C$). A small singlet signal is also observed at 2.2. It was assigned to a methyl group next to a carbonyl group ($H_3C-C=O$) in the reaction mixture.

After 9.5 h of reaction, the sample presented several NMR signals in the aromatic region from 7 to 9 ppm most likely due to the presence of the several aromatic hydrogen atoms in MP, MPO and NP. The four signals assigned to $R-O-CH_3$ decreased in intensity while the other two signals assigned to $C-H$ groups increased (Fig. 9c). Furthermore, the singlet signal assigned to a methyl group next to a carbonyl group ($H_3C-C=O$) was also persistent in the reaction mixture. Upon extended irradiation time, the intensity of the aromatic signals (between 7 and 9 ppm) decreased and they eventually disappeared. These results are indicative that the first steps of the photocatalytic reaction mechanism are several non-destructive modifications of the aromatic ring, which is eventually broken into smaller molecules.

During 1H NMR analysis, it was also observed that photocatalytic reactions in deuterated water are considerably slower than reactions in H_2O . Fig. 10 reports the TiO_2 photocatalytic reaction of a solution of MP (50 ppm) in deuterated water. It can be noticed that at least 5 h are required for 95% MP conversion in D_2O while this can be accomplished in only 3 h in H_2O . The

Table 1
GC–MS retention times (t_R) and spectral characteristics of identified intermediate reaction products of the photocatalytic degradation of methyl parathion

Structure	t_R (min)	Characteristic ions (m/z)
	30.75	$[M]^+ = 263, 233, 216, 200, 139, 125$ methyl parathion, MP
	29.48	$[M]^+ = 247, 230, 215, 185, 170$ methyl paraxon, MPO
	25.22	$[M]^+ = 139, 125, 109, 93, 81$ 4-nitrophenol, NP
	24.44	$[M]^+ = 126, 110, 81, 55$ 1, 2, 4-benzenetriol, BT
	23.29	$[M]^+ = 153, 123, 95, 77$ 4-nitroanisole, NA
	20.70	$[M] = 110, 82, 81, 55$ hydroquinone, HQ
	19.43	$[M] = 128, 100, 65, 50$ aliphatic acid, AA
	14.87	$[M] = 94, 66, 65, 51$ phenol, PH

slower decay of methyl parathion MP is expected given the different role of H₂O and D₂O in the production of the reactive hydroxyl radicals Eqs. (3) and (4).

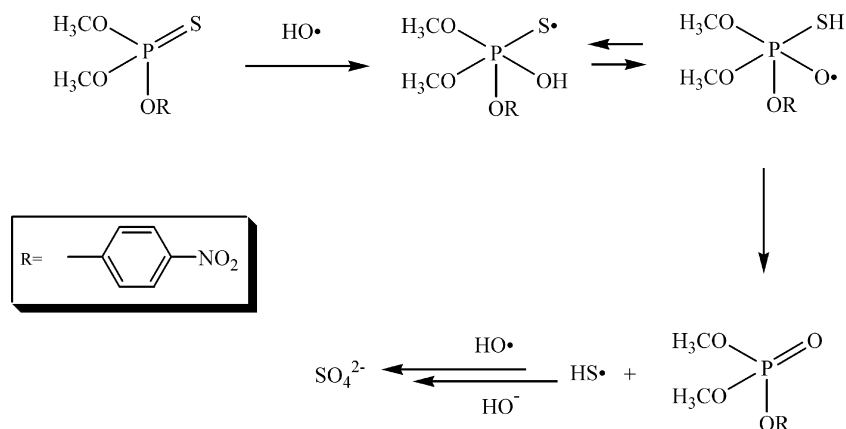
3.4.3. GC–MS analysis

In order to further identify the intermediate organic compounds produced in the photocatalytic degradation of methyl parathion, reaction samples were analyzed by GC–MS. This identification was based on the analysis of standards and by interpretation of fragment ions. Blank analysis helped to discard those peaks coming from the sample handling procedure or formulating agents (when a commercial product was employed). Structures, retention times (*t_R*), and basic ions of the major intermediate compounds detected by GC–MS are given in Table 1. Total ion chromatogram of a sample of the reaction mixture obtained after 1 h of reaction is shown in Fig. 11a. This particular chromatogram shows the presence of methyl parathion (MP), methyl paraoxon (MPO), 4-nitrophenol (NP), 1,2,4-benzenetriol (BT), 4-nitroanisole (NA), and an aliphatic acid (AA) in the reaction mixture. Hydroquinone (HQ) and phenol (PH) in small quantities were also detected by GC–MS analysis in some of reaction mixtures.

Since the photocatalytic degradation of methyl parathion (MP) gives methyl paraoxon (MPO) as an intermediate species, the photocatalytic degradation of MPO under the same reaction conditions was also followed via GC–MS. Total ion chromatogram of a sample withdrawn after 3 h of reaction (Fig. 11b) shows that MPO generates the same intermediate products as methyl parathion (MP) with a strong peak due to low molecular weight aliphatic acid, derived from the oxidation of 1,2,4-benzenetriol. This strong peak was assigned to 5-hydroxymethyl-5H-furfuran-2-one taking as a basis its mass spectrometry pattern. This stable intermediate compound has been previously reported in the photocatalytic degradation of 4-chlorophenol [12].

3.5. Methyl parathion photocatalytic degradation mechanism and overall pathway

Conduction band electrons (e⁻) and valence band holes (h⁺) are generated in an irradiated TiO₂ suspension when



Scheme 3. Oxidation of methyl parathion to methyl paraoxon.

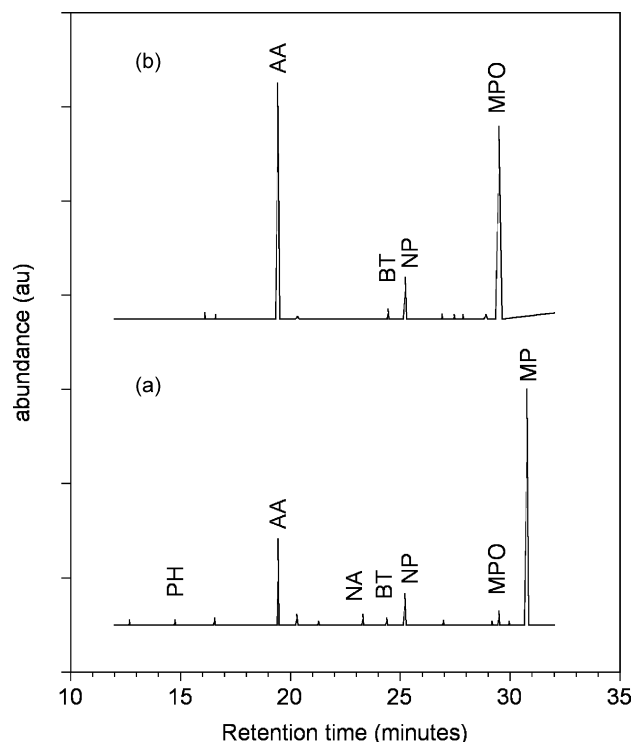
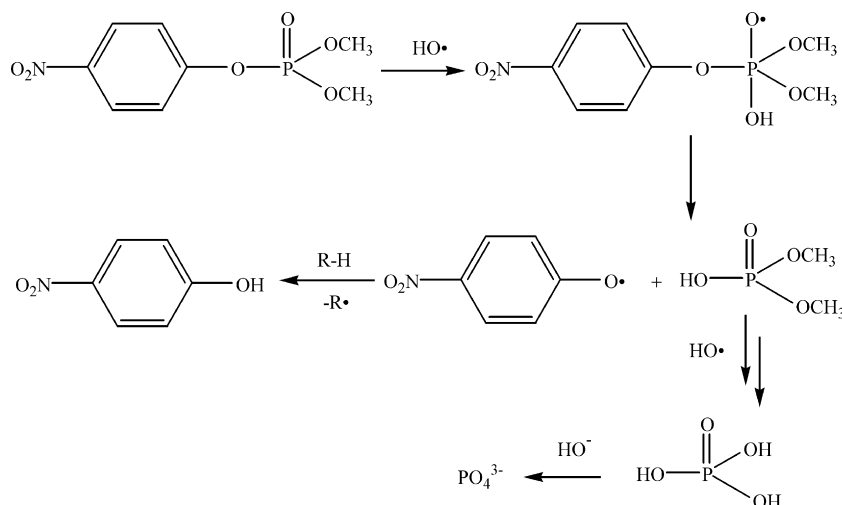


Fig. 11. GC–MS chromatograms obtained for: (a) ethyl acetate extract of a methyl parathion solution ($V=100\text{ mL}$, $C_0=50\text{ ppm}$) irradiated for 1 h with two UV light lamps ($\lambda_{\text{max}}=365\text{ nm}$) in the presence of TiO₂ (0.2 g/100 mL), (b) ethyl acetate extract of a methyl paraoxon solution ($V=100\text{ mL}$, $C_0=59\text{ ppm}$) irradiated for 3.5 h with two UV light lamps ($\lambda_{\text{max}}=365\text{ nm}$) in the presence of TiO₂ (0.2 g/100 mL).

photon energy is larger than its band gap Eq. (1). On this basis, the two possible strong and non-selective oxidating agents result: the photogenerated holes (h⁺) and the resulting hydroxyl radicals (HO[•]). These radicals are generated via oxidation of water by holes or by reaction of hydrogen peroxide Eqs. (3), (4) and (8).

Comparative studies on TiO₂-mediated photocatalytic degradation of several highly methoxylated and hydroxylated benzenes have been reported in literature [42]. The methoxylated compounds give products resulting from hydroxylations and demethylations usually attributed to hydroxyl radical (HO[•]) type



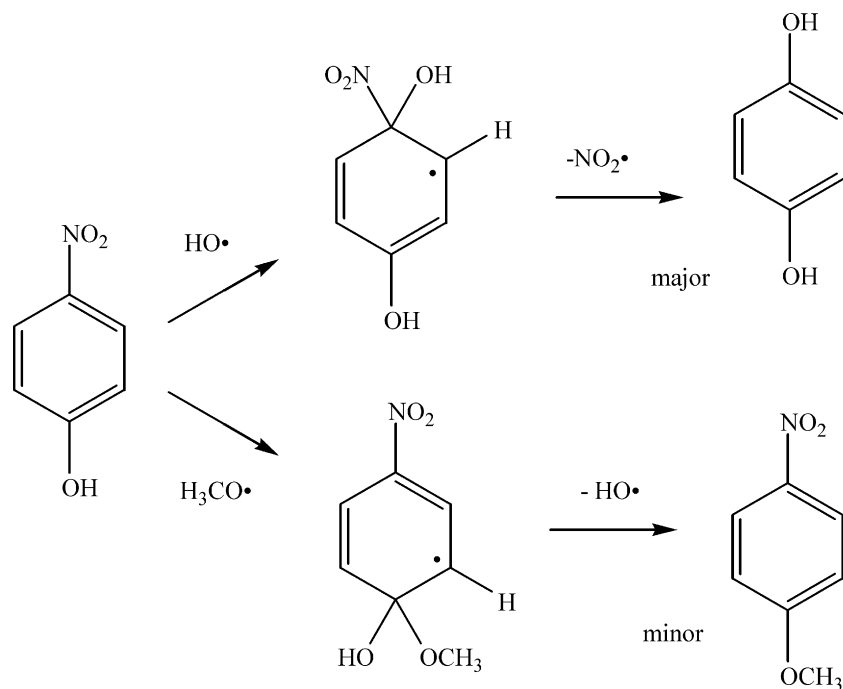
Scheme 4. Oxidation of methyl paraoxon to 4-nitrophenol.

chemistry. Quite different oxidation products are obtained in the case of hydroxylated compounds. It is suggested that hydroxylated compounds are first bound to the TiO_2 surface facilitating electron transfer and subsequent ring-opening oxidation. In the reaction conditions of this study, HO^\bullet radical degradation is expected for most of the reactions involved in the photocatalytic degradation of methyl parathion. However, in the case of some intermediate compounds like 1,2,4-benzenetriol, which can adsorb on TiO_2 surface, an electron transfer mechanism is expected.

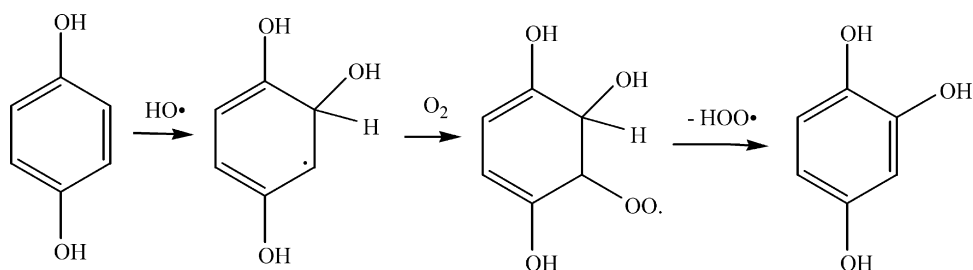
Since the first step in the photocatalytic degradation of methyl parathion is the formation of methyl paraoxon, the most probable pathway must be the addition of HO^\bullet radicals to the phosphorous atom and subsequent elimination of sulfur (Scheme 3). Consistent

with this mechanism, sulfate ions (SO_4^{2-}) were observed to be the first ones produced in the oxidation reaction. In addition, the formation and slow degradation of methyl paraoxon was also noticed. These findings are in clear contrast with the photo Fenton oxidation of methyl parathion, reaction yielding trace amounts of methyl paraoxon only [28]. This distinctive difference can be assigned to the much larger concentrations of HO^\bullet radicals in the Fenton type oxidation.

The formation of 4-nitrophenol from methyl paraoxon is expected after addition of hydroxyl radical (HO^\bullet) to $\text{P}=\text{O}$ bond followed by the elimination of the highly stabilized 4-nitrophenoxy radical (Scheme 4). This mechanism also results in the formation of esters and eventually phosphates that are always present in the product mixture.



Scheme 5. Oxidation of 4-nitrophenol to hydroquinone and 4-nitroanisole.

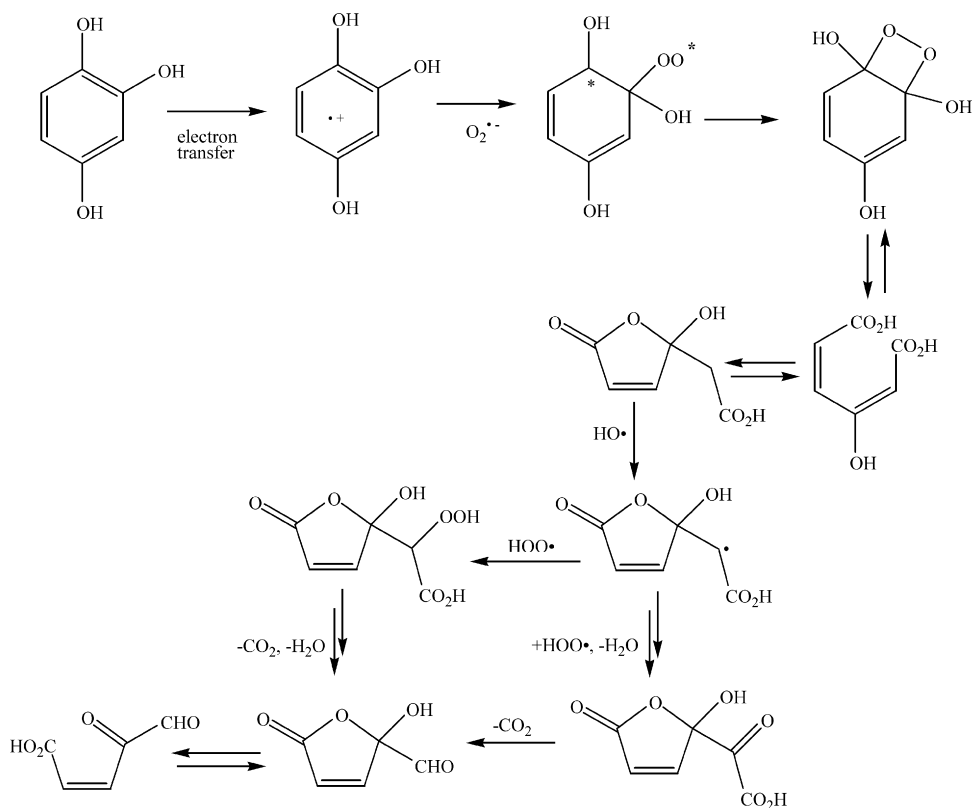


Scheme 6. Oxidation of hydroquinone to 1,2,4-benzenetriol.

The mechanistic pathway for the degradation of *para*-substituted phenols has been described in a number of contributions [5,43–45]. More specifically, the photocatalytic degradation of 4-chlorophenol leads to significant number of intermediates species [12,13]. In this respect, several parallel reaction pathways were proposed for the oxidation of this aromatic compound. All previous reports have shown that there are two major chemical transformations that compete in the degradation of 4-nitrophenol; hydroxyl radical $\text{HO}\cdot$ substitution to form hydroquinone and hydroxylation to form 4-nitrocatechol. Under the reaction conditions studied, the dominant formation of hydroquinone with trace amounts of 4-nitrocatechol was observed. The aromatic compound, 4-nitroanisole, was also detected by GC–MS analysis during the photocatalytic degradation of both MP and MPO. This intermediate compound could be also formed via a reaction mechanism (Scheme 5) involving radical intermediates [12,13,42].

Studies in the photocatalytic degradation of hydroquinone by several researchers [12,13] and now ourselves clearly seem to indicate that benzoquinone may not be an important intermediate since it is not a detectable species. Furthermore, oxidation of hydroquinone to 1,2,4-benzenetriol is believed to occur by addition of $\text{HO}\cdot$ with subsequent reaction with O_2 and elimination of the $\text{HOO}\cdot$ radical [12] as described in Scheme 6. Only a small amount of hydroquinone has been shown to undergo ring opening and subsequent hydroxylation appears to be by far the major path of degradation.

In the case of 1,2,4-benzenetriol, it has been proposed that its photocatalytic degradation proceeds by electron transfer to give a radical cation that undergoes subsequent oxidation with ring cleavage to produce low molecular weight acids [12]. This electron transfer mechanism is facilitated by initial adsorption of this triol on the surface of the TiO_2 catalyst [48,49]. The photocatalytic degradation of both, methyl parathion and



Scheme 7. Oxidation of 1,2,4-benzenetriol to 5-hydroxymethyl-5H-furfuran-2-one.

methyl paraoxon, gave a simple degradation pattern monitored by GC–MS. It is interesting to realize that a particular low molecular weight carboxylic acid, 5-hydroxymethyl-5H-furfuran-2-one, was preferentially formed in the oxidation of both organic compounds. These experimental results show that the photocatalytic oxidation of 1,2,4-benzenetriol favored a particular pathway (Scheme 7) in contrast to previous observations in which this triol was considered to follow several other oxidation steps [12,13].

4. Conclusions

The results of the present study clearly indicate that the first step of the photocatalytic degradation of methyl parathion (MP) is its oxidation to methyl paraoxon (MPO). This first step involves weakly adsorbed MP species not affected by the pH of the water solution. On the other hand, the photocatalytic oxidation of methyl paraoxon is strongly influenced by the acidity of the solution. Therefore, the overall conversion of total organic carbon is also affected by pH. Under alkaline conditions, only 60% of the TOC is converted to CO₂ after 6 h of reaction. At low pH, 90% of TOC is converted to CO₂ in the same time.

The observed reaction mechanism, as evidenced by GC–MS, involves methyl paraoxon species transformed into hydroquinone further oxidized to benzenetriol with these species undergoing selective oxidation to a low molecular weight aliphatic acid, 5-hydroxymethyl-5H-furfuran-2-one. Aliphatic acids are further degraded to lower molecular weight carboxylic acids transformed in the final step into CO₂. Considering all facts described above and given major organic intermediate compounds and inorganic ions identified during the photocatalytic degradation of methyl parathion one can confirm the mechanistic degradation pathway presented in Scheme 2 of this study.

In addition, it is confirmed that the photocatalytic degradation of MP in deuterated water takes place at slower rates indicating that water is indeed involved in the production of hydroxyl radicals and that DO• radicals are generated at a slower pace than HO• radicals.

Acknowledgements

Financial support from CONACyT (Grant 28253-U, Grant C01-45936 and fellowship 144673) is gratefully acknowledged. Titanium oxide was kindly donated by Degussa Corporation. The authors thank Dr. Deogracia Ortiz-Pérez, who is a professor at the Universidad Autónoma de San Luis Potosí, for her help with the GC–MS analysis.

References

- [1] H. de Lasa, B. Serrano, M. Salices, Photocatalytic Reaction Engineering, Springer, New York, 2005.
- [2] O. Carp, C.L. Huisman, A. Reller, Prog. Solid State Chem. 32 (2004) 33–177.
- [3] K. Kabra, R. Chaudhary, R.L. Sawheney, Ind. Eng. Chem. Res. 43 (2004) 7683–7696.
- [4] O. Legrini, E. Oliveros, A.M. Braun, Chem. Rev. 93 (1993) 671–698.
- [5] E. Leyva, E. Moctezuma, M.G. Ruiz, L.M. Torres-Martínez, Catal. Today 40 (4) (1998) 367–376.
- [6] Y. Oh, X. Li, J.W. Cabbage, W.S. Jenks, Appl. Catal. B: Environ. 54 (2004) 105–114.
- [7] E. Moctezuma, E. Leyva, E. Monreal, N. Villegas, D. Infante, Chemosphere 39 (3) (1999) 511–517.
- [8] D. Chen, A.K. Ray, Water Res. 32 (11) (1998) 3223–3234.
- [9] M. Canle L, J.A. Santaballa, E. Vulliet, J. Photochem. Photobiol. A: Chem. 175 (2005) 192–200.
- [10] P.F. Schwarz, N.J. Turro, S.H. Bossmann, A.M. Braun, A.M.A.A. Wahab, H. Dürr, J. Phys. Chem. B 101 (1997) 7127–7134.
- [11] C.D. Jaeger, A.J. Bard, J. Phys. Chem. 83 (1979) 3146–3152.
- [12] X. Li, J.W. Cabbage, T.A. Tetzlaff, W.S. Jenks, J. Org. Chem. 64 (1999) 8509–8524.
- [13] X. Li, J.W. Cabbage, W.S. Jenks, J. Org. Chem. 64 (1999) 8525–8536.
- [14] L. Cermenati, P. Pichat, C. Guillard, A. Albini, J. Phys. Chem. B 101 (1997) 2650–2658.
- [15] R. Terzian, N. Serpone, M.A. Fox, J. Photochem. Photobiol. A: Chem. 90 (1995) 125–135.
- [16] L. Amalric, C. Guillard, P. Pichat, Res. Chem. Intermed. 21 (1) (1995) 33–46.
- [17] P. Piccinini, C. Minero, M. Vicenti, E. Pelizzetti, Catal. Today 39 (1997) 187–195.
- [18] D. Bahnemann, Solar Energy 77 (2004) 445–459.
- [19] J. Fournier, Chemie des Pesticides, Editions Cultures et Techniques, Nantes, 1988.
- [20] J.R. Chambers, H.W. Chambers, in: L. Somasundaraman, J.R. Coats (Eds.), Pesticide Transformation Products, ACS Symp. Ser., 1991.
- [21] K. Harada, T. Hisanaga, K. Tanaka, New J. Chem. 11 (8/9) (1987) 597–600.
- [22] K. Harada, T. Hisanaga, K. Tanaka, Water Res. 24 (1990) 1415–1417.
- [23] H.D. Burrows, M. Canle L, J.A. Santaballa, S. Steenken, J. Photochem. Photobiol. B: Biol. 67 (2002) 71–108.
- [24] H. Roques, Chemical Treatment: Principles and Practice, VCH, New York, 1996.
- [25] B.D. Cavell, Pestic. Sci. 10 (1979) 177–181.
- [26] P. Meallier, J. Nury, B. Pouyet, C. Coste, J. Bastide, Chemosphere 12 (1977) 815–818.
- [27] E. Gal, P. Aires, E. Chamarro, S. Esplugas, Water Res. 26 (7) (1992) 911–915.
- [28] J.J. Pignatello, Y. Sun, Water Res. 29 (8) (1995) 1837–1844.
- [29] K.E. O'Shea, S. Beightol, I. Garcia, M. Aguilar, D.V. Kalen, W.J. Cooper, J. Photochem. Photobiol. A: Chem. 107 (1997) 221–226.
- [30] S. Malato, J. Blanco, C. Richter, B. Milow, M.I. Maldonado, Chemosphere 38 (5) (1999) 1145–1156.
- [31] R. Doong, W. Chang, J. Photochem. Photobiol. A: Chem. 107 (1997) 239–244.
- [32] M. Kerzhentsev, C. Guillard, J.-M. Herrmann, P. Pichat, Catal. Today 27 (1996) 215–220.
- [33] J.K. Konstantinou, T.M. Sakellarides, V.A. Sakkas, T.A. Albanis, Environ. Sci. Technol. 35 (2001) 398–405.
- [34] V.A. Sakkas, D.A. Lambropoulou, T.M. Sakellarides, T.A. Albanis, Anal. Chim. Acta 467 (2002) 233–243.
- [35] A. Sanjuán, G. Aguirre, M. Alvaro, H. García, Water Res. 34 (1) (2000) 320–326.
- [36] G. Palestino, MS Thesis, UASLP, México, 2001.
- [37] E. Leyva, E. Moctezuma, G. Palestino, Book of Abstracts, in: Proceedings of the 221st ACS National Meeting, Org Part 2, 2001, p. 287.
- [38] E. Leyva, E. Moctezuma, H. Zamarripa, Rev. Intern. Contam. Amb. 19 (3) (2003) 115–125.
- [39] J. Medina-Valtierra, E. Moctezuma, M. Sánchez-Cárdenas, C. Frausto-Reyes, J. Photochem. Photobiol. A: Chem. 174 (2005) 246–252.
- [40] C. Minero, F. Catozzo, E. Pelizzetti, Langmuir 8 (1992) 481–486.
- [41] M.I. Franch, J.A. Ayllón, J. Peral, X. Domenech, Catal. Today 76 (2002) 221–233.
- [42] X. Li, J.W. Cabbage, W.S. Jenks, J. Photochem. Photobiol. A: Chem. 143 (2001) 69–85.

- [43] V. Augugliaro, L. Palmisano, M. Schiavello, A. Sclafani, L. Marchese, G. Martra, F. Miano, *Appl. Catal.* 69 (1991) 323.
- [44] M.S. Dieckmann, K.A. Gray, *Water Res.* 30 (5) (1996) 1169–1183.
- [45] N. San, A. Hatipoglu, G. Koçtürk, Z. Çinar, *J. Photochem. Photobiol. A: Chem.* 146 (2002) 189–197.
- [46] K.L. Hadjivanov, D.G. Kissurk, A. Davidov, *J. Catal.* 116 (2) (1989) 498–505.
- [47] D.L. Pavia, G.M. Lampman, G.S. Kriz, *Introduction to Spectroscopy*, Harcourt College Pub, New York, 2001.
- [48] J. Cunningham, P. Sedlak, *J. Photochem. Photobiol. A: Chem.* 77 (1994) 255–263.
- [49] A. Mills, S. Morris, *J. Photochem. Photobiol. A: Chem.* 71 (1993) 75–83.